Supplementary Information

Dynamic regulation of Pep-induced immunity through post-translational control of defense transcript splicing

Keini Dressano[1], Philipp R Weckwerth[1], Elly Poretsky[1], Yohei Takahashi[1], Carleen Villarreal[1], Zhouxin Shen[1], Julian I. Schroeder[1], Steven P. Briggs[1], Alisa Huffaker[1]*

Affiliations

[1]Section of Cell and Developmental Biology, UC San Diego, California, United States.

*Correspondence to: Alisa Huffaker, ahuffaker@ucsd.edu

This PDF file includes:

1. **Supplementary Methods**
2. **Supplementary Figures 1-24**
3. **Supplementary References 73-80**

1. Supplementary Methods

Generation of constructs and plant materials

The *IRR* gene and its endogenous promoter sequence was amplified from the genomic DNA of *Arabidopsis thaliana* using standard PCR. To generate the IRR phosphoabolishing mutant, the QuickChange II XL site-directed mutagenesis kit (Agilent Technologies) was used to substitute serine to alanine (S745A, S747A), following manufacturer's instructions. The PCR fragments were first cloned into the pENTR/D-TOPO vector, and transferred by recombination into plant vectors. The *IRR* PCR fragment was transferred into pGWB441 and pGWB414 vectors. The endogenous promoter and coding-region of *IRR* (pIRR-IRR) were transferred into pGWB440 vector. The *SR45* and CC1-*splicing factor* coding regions were amplified from Arabidopsis cDNA using standard PCR, cloned into the pENTR/D-TOPO vector and transferred by recombination into pGWB441 and pGWB414 vectors. To generate pCPK28:CPK28 constructs, the promoter sequence was amplified from Arabidopsis genomic DNA by PCR and cloned into pXCS-YFP vector into *Asc*I/*Hind*III sites. Synthetic cDNA encoding either canonically spliced *CPK28* or the *CPK28*-RI splice variant were made by Genscript were amplified by PCR and cloned into the pXCS-YFP vector carrying the CPK28 promoter into *Hind*III/*Eco*RI sites. Alternatively, the pCPK28:CPK28 fragment was cloned into the pENTR/D-TOPO vector and transferred by recombination into pGWB440. Primers used to amplify all fragments are shown in Supplementary Table 4. All constructs were verified by DNA sequencing and transformed into *Agrobacterium tumefaciens* strain GV3101. The constructs were either expressed transiently in *Nicotiana benthamiana* through infiltration with *A. tumefaciens*, as previously described[73], or into

Arabidopsis plants via *Agrobacterium tumefaciens* by floral-dip method[74]. Transgenic lines from the T2 and T3 generation were used in the experiments. *A. thaliana* ecotype Columbia-0 was used as wild-type. The mutants *irr-1* (SALK_015201), *irr-2* (SALK_066572), *sr45* (SALK_123442) and *cpk28* (WiscDsLox264D03) were acquired from the Arabidopsis Biological Resource Center, ABRC[75].

Growth conditions

Arabidopsis thaliana seeds were surface-sterilized in chlorine (Cl_2) gas (vapor-phase). Sterilized seeds were stratified for 3 days at 4 °C and then germinated on plates containing half-strength MS[76] medium without sucrose and vitamins (PhytoTechnology Laboratories), adjusted to pH 5.7 using KOH with or without 0.8% phytagel (PhytoTechnology Laboratories). For subsequent experiments, seedlings were either maintained on plates or transferred to soil as indicated. Arabidopsis, maize var. B73 and *Nicotiana benthamiana* plants were grown in a growth room (16 h light, 150 μmol $m^{-2}s^{-1}$ and 8 h dark, or 12h light and 12h dark) at 22 ± 2 °C.

Phylogenetic tree of Arabidopsis RNA-binding proteins

The phylogenetic tree was calculated using the Maximum Likelihood method in MEGA7[77, 78]. The bootstrap consensus tree inferred from 5000 replicates using the Nearest-Neighbor-Interchange method was taken to represent the phylogenetic relationship of a subset of 30 RNA-binding proteins in Arabidopsis. All positions containing gaps and missing data were eliminated. Evolutionary analyses were conducted in MEGA7[78].

Root growth inhibition

Sterile seeds were sown on either half-strength MS media or half-strength MS media supplemented with concentrations of either 0.1 or 1 μM peptide and plates oriented vertically in the for growth in chambers. Primary root length was measured after 15 days and the percent root growth on AtPep1 versus standard half-strength MS media was calculated for each line.

Reactive Oxygen Species (ROS) assay

Peptide-induced ROS production in leaf discs from four-week-old plants was measured continuously for 40 min via light emission from luminol oxidized by horseradish peroxidase in the presence of H_2O_2 using an automated plate reader with luminescence filter as described previously[79]. The concentration of peptide used is indicated in each figure. Water was used as control treatment.

Gene expression analysis

Sterile seeds were sown on half-strength MS media for 7-10 days and transferred to 24-well plates containing liquid half-strength MS. Approximately 15 plants were transferred to individual wells. Three hours after transfer, plants were treated with either water or a solution of 1 μM peptide for 24 hours (unless indicated otherwise) at room temperature and constant light. Plant tissue was

harvested in liquid nitrogen, and total RNA was isolated using Trizol reagent and treated with DNAse according to the manufacturer's instructions (Life Technologies). The cDNA was synthesized using the M-MLV Reverse Transcriptase (Thermo Fisher Scientific) and 1-2 µg of RNA. 1-1.5 µL cDNA was used for RT-PCR reactions. The qRT-PCR analysis was performed using 3-fold diluted cDNA, SsoAdvanced(tm) Universal SYBR(R) Green Supermix (Bio-Rad) and a StepOne Real-Time PCR System (Applied Biosystems). Based on the threshold cycle (Ct) value, ΔCt was calculated relative to either glyceraldehyde 3-phosphate dehydrogenase (*GAPDH*) or *ACTIN2,* and fold-change calculated relative to the average expression of control genotypes or treatments as indicated in figure legends. The genes analyzed and primers used in these experiments are shown in Supplementary Table 4.

Confocal analysis

Leaf disks from *Nicotiana benthamiana* transiently expressing YFP-fusions of proteins of interest were visualized using confocal microscopy (Olympus FV1000). The wavelengths for YFP excitation and emission were 514 nm and 527 nm, respectively. Image processing was completed using Image J.

***Pseudomonas syringae* infection**

Pseudomonas syringae pv. *tomato* DC3000 (*Pst*) was grown in liquid low-salt LB medium containing 50 µg/mL rifampicin until their optical density, OD_{600}, was approximately 1.0. Bacterial cells were diluted in 10 mM $MgCl_2$ to the OD_{600} of 0.2, and the solution was diluted again 1000-fold (to yield 10^5 colony forming units/mL) in 10 mM $MgCl_2$. Using a needleless syringe, four-week-old Arabidopsis leaves were infiltrated with the diluted bacterial solution on the abaxial surface. After infiltration, plants were kept in dome-covered trays to maintain a humid environment. Each sample collected was comprised of two 6 mm-diameter leaf disks collected from the same leaf, with each sample group including single leaves from six to eight different individual plants. Individual samples were collected and homogenized in 10 mM $MgCl_2$, and serial dilutions were made and plated on solid low salt LB media supplemented with 50 µg/mL rifampicin and 12.5 µg/mL cycloheximide. After 2-3 days at 28°C, the resulting colonies were counted manually.

***Botrytis cinerea* infection**

Botrytis cinerea was grown on V8 juice agar plates supplemented with $CaCO_3$ (9 g/L) for 8 days at room temperature. The spores were harvested, resuspended in BD Difco Potato Dextrose Broth (Becton, Dickinson and Company) containing 0.1% Tween at a density of 1 to 5×10^5 spores/mL, and incubated for 2 hours at 25-28°C with gentle shaking before inoculation. For inoculation, leaves of four-week-old plants were wounded with a needle, and a 5 µL aliquot of suspended spores was applied to the adaxial surface of the wound site. Symptoms were monitored for 4 days, and the infection was analyzed by measuring both the lesion diameter, and the fungal colonization in leaves using qRT-PCR quantification of fungal *CUTINASE* DNA (Z69264) relative to an Arabidopsis reference gene, as described previously[80].

Statistical Analyses

Statistical analyses were performed using GraphPad Prism 8.0 (GraphPad Software, Inc.). Student's unpaired t-tests were used for pairwise comparisons. One-way analyses of variance (ANOVAs) were used to evaluate statistical differences. Tukey tests were performed to correct for multiple comparisons between the groups. P values < 0.05 were considered statistically significant.

2. Supplementary Figures

a

Phosphopeptide	Unique Peptide	Protein Coverage	Accession	Water treatment				Pep treatment				p-value
				rep 1	rep 2	rep 3	rep 4	rep 1	rep 2	rep 3	rep 4	
sKsLDEDYDMK	31	0.1519757	AT3G23900.3	30.7	37.5	33.42	23.38	19.11	20.37	21.34	23.95	0.02
SGSPSsPTRR, SGsPSSPTRR	3	0.0194805	GRMZM2G132936	0.87	0	0.71	1.38	0	0	0	0	0.04

b

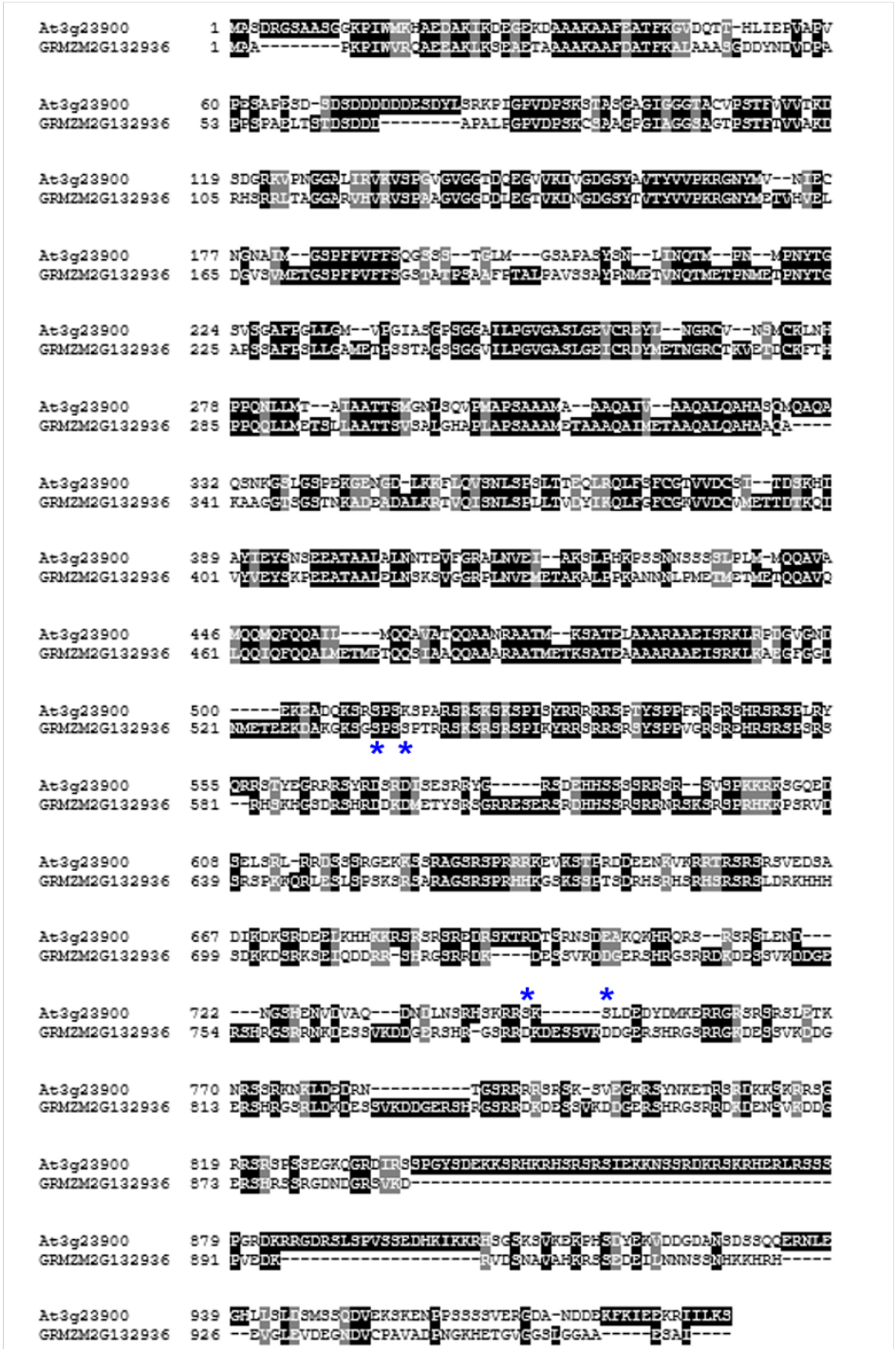

Supplementary Figure 1. IRR phosphopeptides detected in Arabidopsis and maize. a, IRR phosphopeptides detected in Arabidopsis and maize suspension cells 10 min after treatment with solutions of either 100 nM AtPep1 and ZmPep3 (Pep), respectively as compared to water. The serine (S) residues that were dephosphorylated after peptide treatment are shown as lower case (s) in the phosphopeptide fragments shown. Four biological replicates were analyzed. **b,** Sequence alignment of *IRR* in Arabidopsis and maize showing the phosphorylation sites detected by phosphoproteomic analysis after Pep treatment. The serine (S) residues that were dephosphorylated after peptide treatment are denoted by blue stars. Letters with gray background indicate similar amino acids, black background, identical.

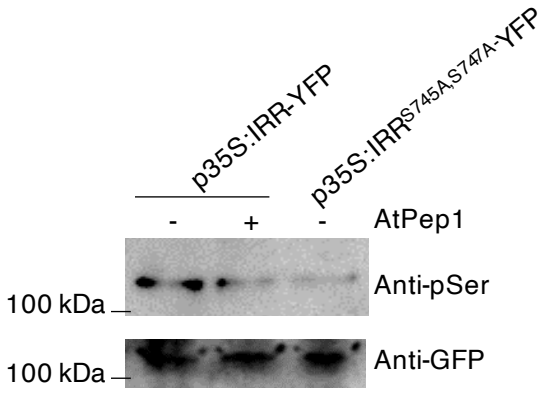

Supplementary Figure 2. Confirmation of AtPep1-induced phosphorylation of IRR. Transgenic plants overexpressing either IRR-YFP or IRR^{S745A,S747A}-YFP were treated with water or a 1 μM solution of AtPep1 for 30 min. Total protein was extracted from whole seedlings, and subjected to immunoblot analysis with anti-phospho-Ser (anti-pSer) antibody. Immunoblot analysis with anti-GFP and anti-HA antibodies were used to visualize protein loading. The experiment was repeated at least two times independently, with similar results.

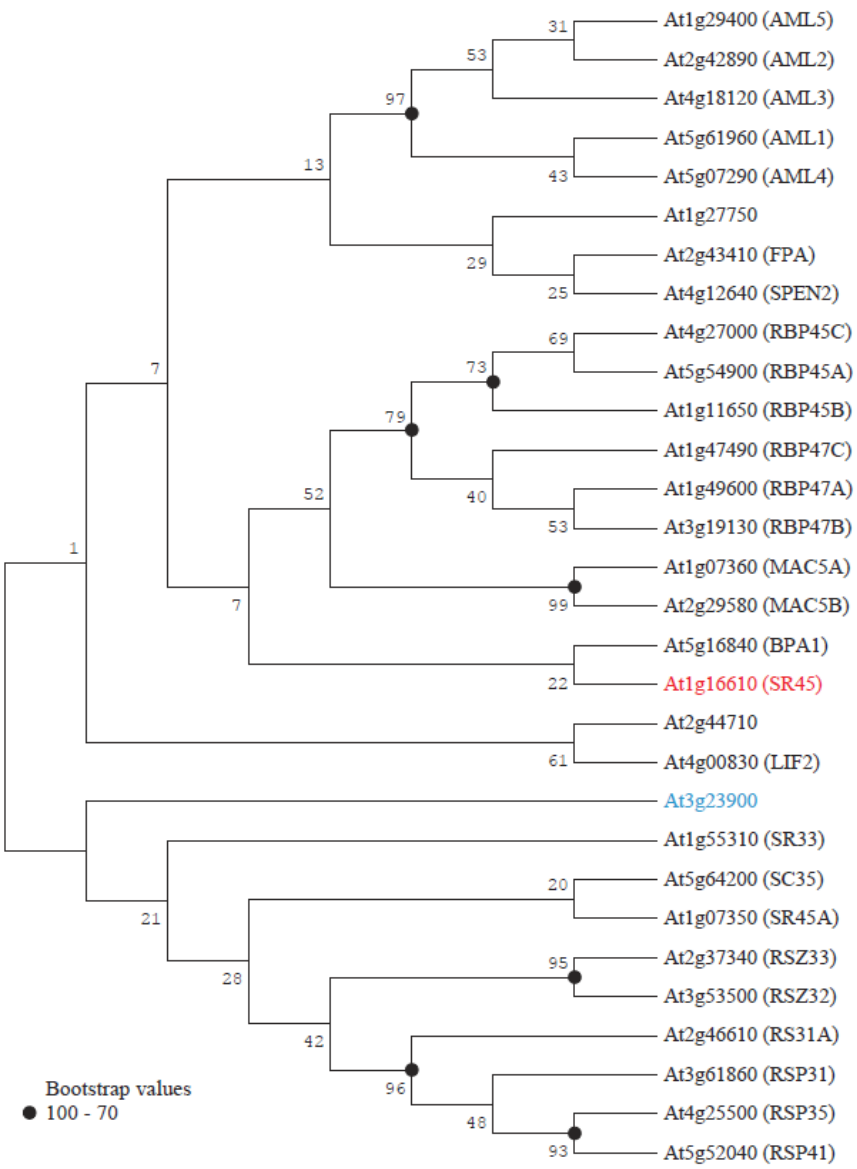

Supplementary Figure 3. Phylogenetic tree of a subset of 30 Serine/Arginine-rich (SR) RNA-binding proteins in Arabidopsis. The phylogenetic tree was calculated using the Neighbor-joining method in MEGA7. The bootstrap consensus tree inferred from 5000 replicates using the Nearest-Neighbor-Interchange method was taken to represent the phylogenetic relationship of 30 RNA-binding proteins in Arabidopsis. IRR, At3g23900 (blue) and SR45 (red) are highlighted.

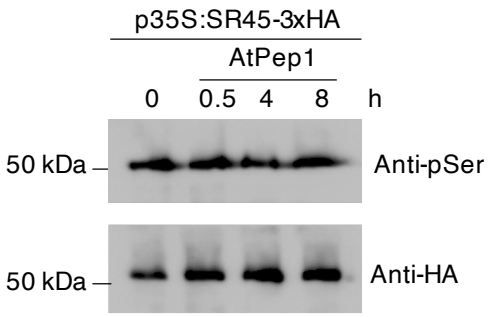

Supplementary Figure 4. Analysis of SR45 phosphorylation after AtPep1 treatment. Plants expressing p35S:SR45-3xHA were treated with 1 µM AtPep1 for 0, 0.5, 4 and 8 hours (h). Total protein was extracted from whole seedlings, and subjected to immunoblot analysis with anti-phospho-Ser (anti-pSer) antibody. Immunoblot analysis with anti-HA antibody was used to show protein loading. This experiment was repeated two times independently, with similar results.

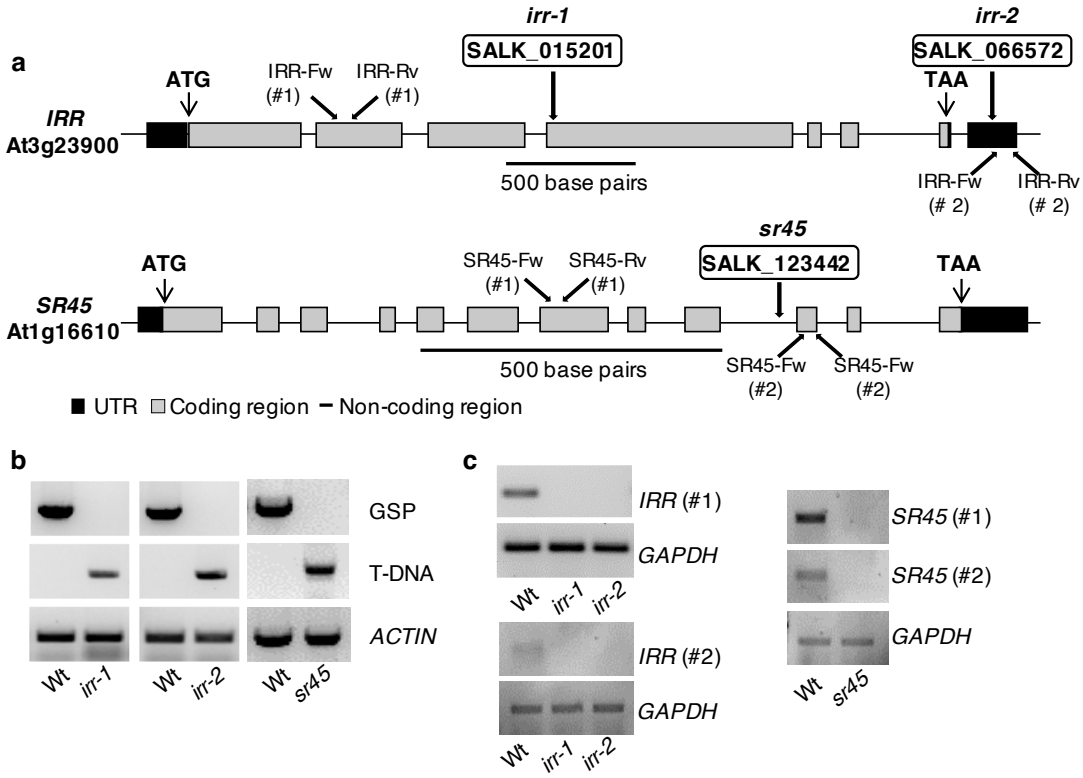

Supplementary Figure 5. Validation of *IRR* and *SR45* T-DNA insertion lines. a, T-DNA insertion sites of the knockout lines, *irr-1* (SALK_015201)*, irr-2* (SALK_066572) *and sr45* (SALK_123442). UTR, untranslated region. **b,** Analyses of the T-DNA insertion in the *Arabidopsis* genome of the lines *irr-1, irr-2* and *sr45.* GSP, amplification products of a PCR reaction using two gene specific primers. T-DNA, amplification products of a PCR reaction using the T-DNA specific primer LBb1.3 and one gene specific primer. The detection of the *ACTIN* gene was used as internal control. **c,** RT-PCR analyses to validate *irr-1, irr-2* and *sr45* mutants. *GAPDH* gene expression was used as internal control.

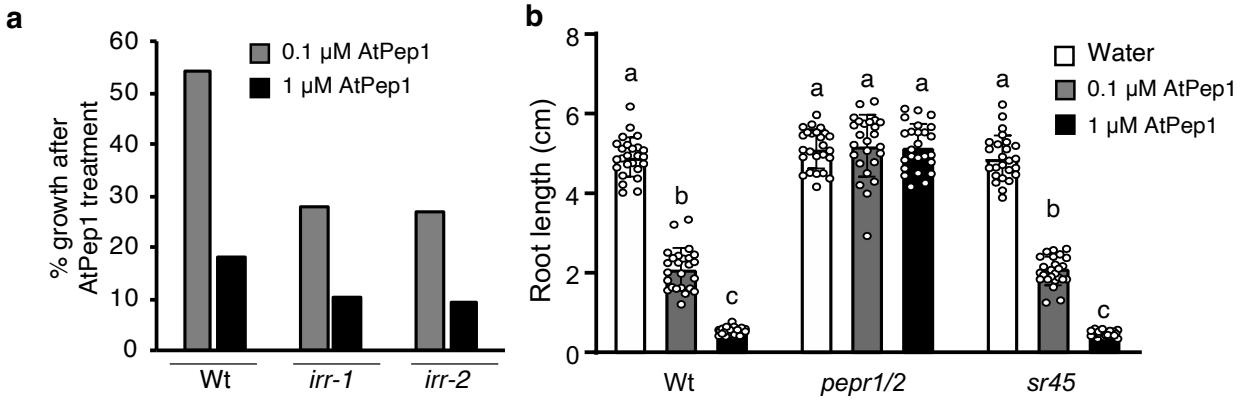

Supplementary Figure 6. Root elongation of *irr* and *sr45* mutants in response to AtPep1. a, Percent root growth of wild-type (Wt), *irr-1* and *irr-2* mutants grown on medium supplemented with AtPep1 as compared plants on standard medium. **b,** Wt, *pepr1/pepr2* (*pepr1/2*) and *sr45* mutants were treated with water or AtPep1. n=17-25 plants. Error bars indicate mean ± SD. Different letters represent significant differences (one-way ANOVA followed by Tukey's test corrections for multiple comparisons; $P < 0.05$). Primary root length was measured after 15 days of treatment.

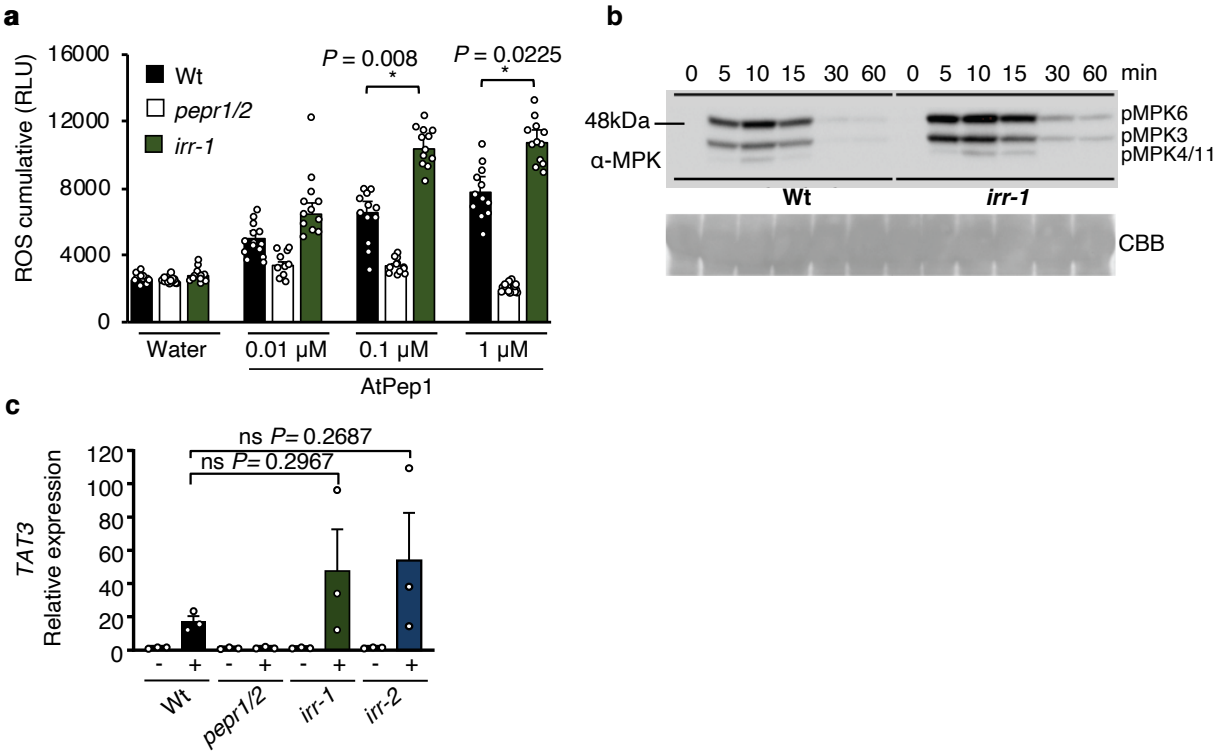

Supplementary Figure 7. *IRR* mutants are hypersensitive to AtPep1. a, Total ROS production was registered continuously using luminol fluorescence for 40 min after addition of 0, 0.01, 0.1 and 1 µM AtPep1, then summed. Wt, wild-type; *pepr1/2*, *pepr1/pepr2*. n = 12, error bars represent SEM. The asterisk indicates significant differences using Student t-tests (two-tailed distribution, unpaired), with $P < 0.05$; ns, not significant. **b,** MAP Kinase 3, 6, 4 and 11 (MPK3/6/4/11) phosphorylation analysis. Seedlings were treated with a 1 µM solution of AtPep1 for 0, 5, 10, 15, 30 or 60 min. MPK3/6/4/11 phosphorylation was detected by immunoblotting using an anti-phospho-p44/42 MAPK antibody. The immunoblot was probed with Coomassie Brilliant Blue (CBB) to determine equal loading. **c,** The relative expression level of the AtPep1-inducible gene *TAT3* was determined by real-time qRT-PCR using mRNA from whole seedlings treated with either water (-) or a 1 µM solution of AtPep1 (+) for 24 h. Values represent the fold-change in *TAT3* expression versus the water-treated wild-type (Wt) control samples after normalization against *GAPDH* expression. Error bars indicate the SD of three biological replicates. ns, not significant (Student t-tests, two-tailed distribution, unpaired). Experiments in a-c were repeated three times independently, with similar results.

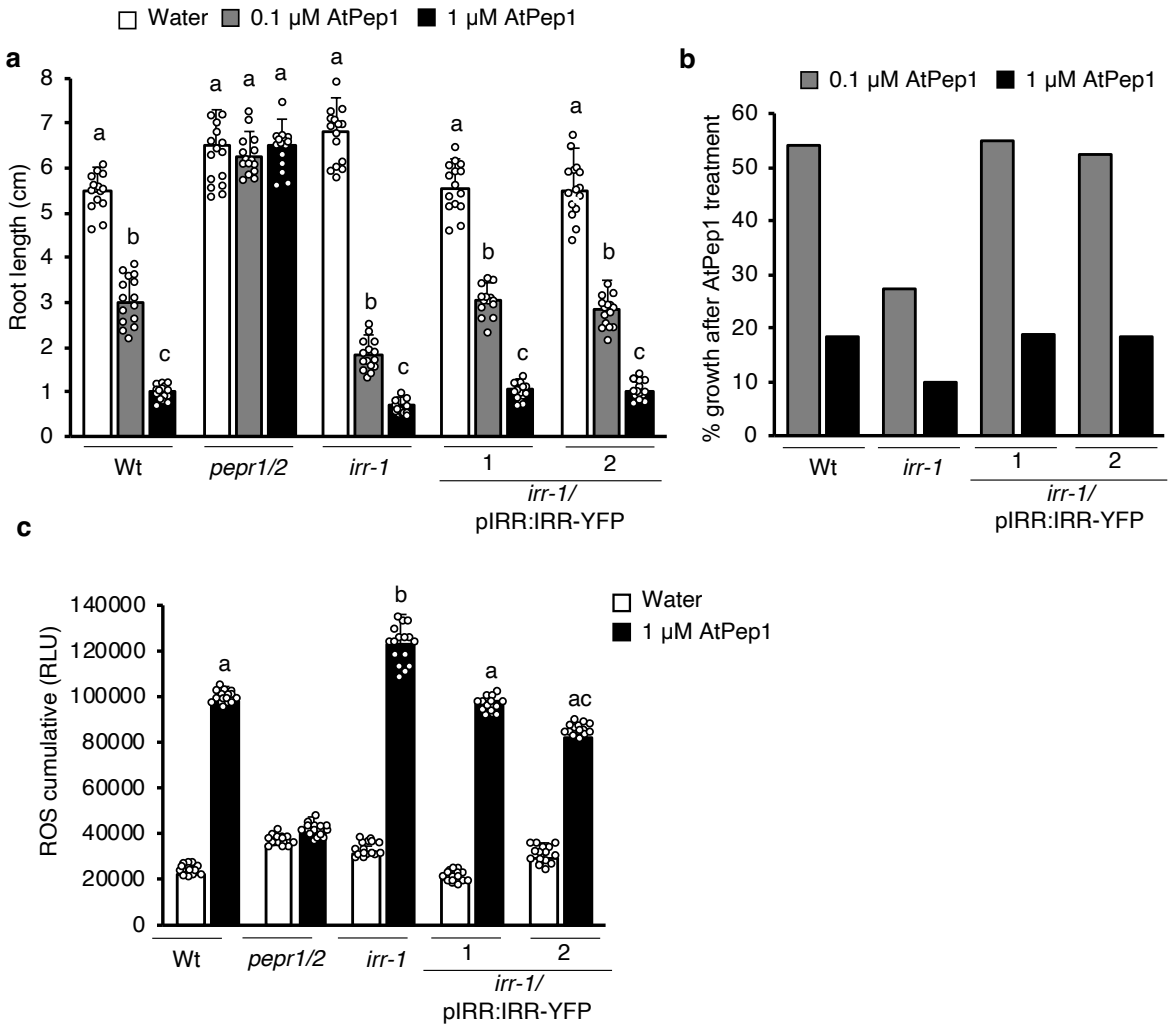

Supplementary Figure 8. The *IRR* gene driven by its native promoter complements the *irr-1* mutant phenotype. a, Root length of Arabidopsis seedlings after treatment with water or AtPep1 (0.1 µM and 1 µM). Roots were measured after 15 days of treatment, n = 15. Error bars indicate represent SD. **b,** Percentage of root growth after peptide treatment. The data from one representative experiment is shown. **c,** Total ROS production was registered continuously using luminol fluorescence for 40 min after addition of 0 or 1 µM AtPep1, then summed, n=16. Error bars represent SD. Different letters represent significant differences (one-way ANOVA followed by Tukey's test corrections for multiple comparisons; $P < 0.05$). Two independent complementation lines of pIRR:IRR-YFP (1 and 2) were analyzed. Wild-type (Wt) and *pepr1/pepr2* (*pepr1/2*) were used as controls. Experiments in a-c were repeated three times independently, with similar results.

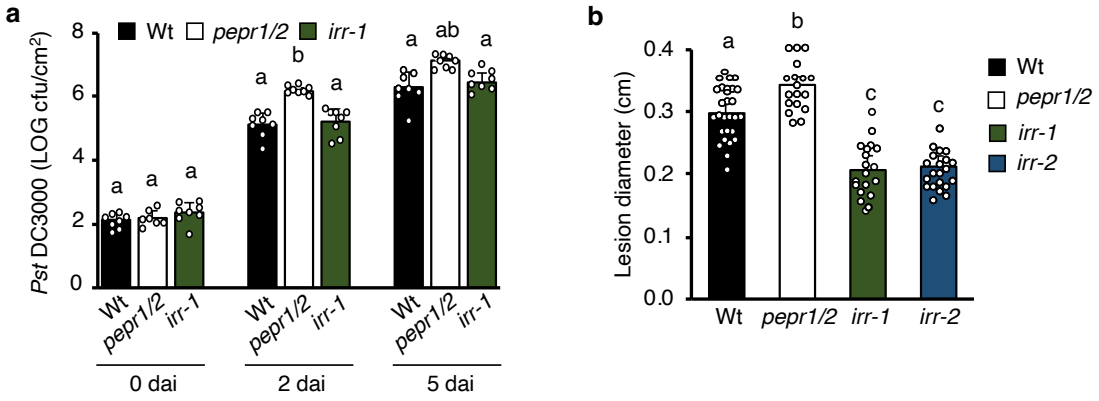

Supplementary Figure 9. *Pst* DC3000 and *Botrytis cinerea* infection assays to assess basal resistance of *irr* knockout lines. a, *Pst* DC3000 infection assay of wild-type (Wt), *pepr1/pepr2 (pepr1/2)* and *irr-1* plants. Bars indicate bacterial growth 0, 2 and 5 days after inoculation (dai). Error bars indicate SEM, n = 8. **b,** *Botrytis cinerea* infection in Wt, *pepr1/2* and *irr* mutants. The lesion diameter in leaves was measured 4 days after infection. Error bars indicate SEM, n = 17-28. Different letters represent significant differences (one-way ANOVA followed by Tukey's test corrections for multiple comparisons; $P < 0.05$). Experiments in a,b were repeated three times independently, with similar results.

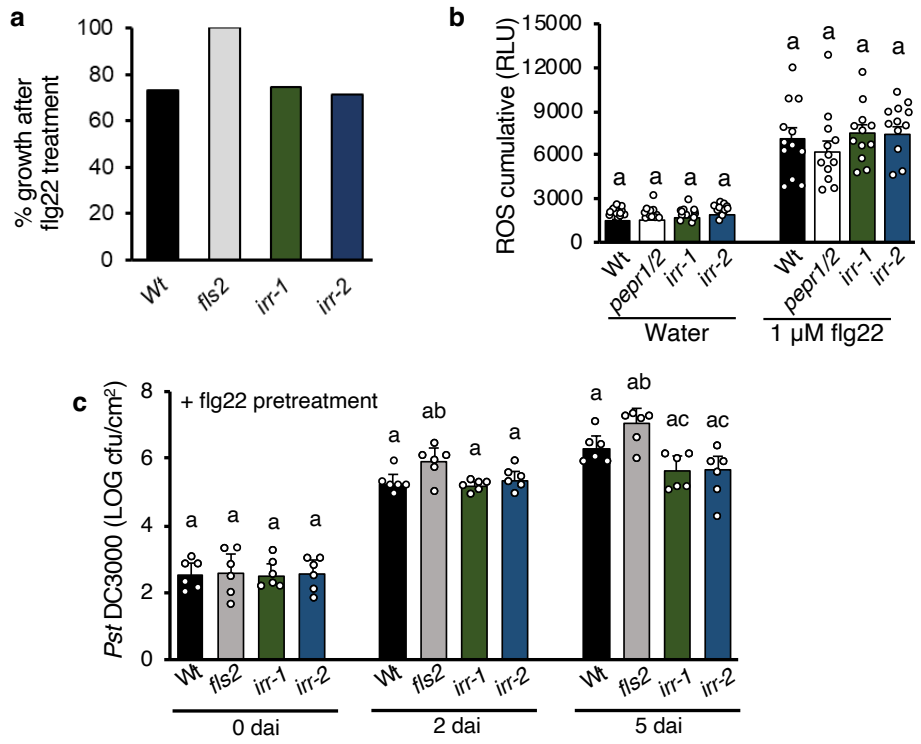

Supplementary Figure 10. flg22-induced responses in *irr* mutants. a, Percent root growth of wild-type (Wt), *irr-1, irr-2* and *fls2* mutants when grown in the presence of 0.1 µM flg22 as compared to plants on standard medium, n = 10 **b,** Total ROS production was registered continuously using luminol fluorescence for 40 min after addition of 1 µM flg22, then summed. Wt and *fls2* were used as controls, n = 12, error bars represent SEM. **c,** *Pst* DC3000 infection assay of Wt, *fls2, irr-1* and *irr-2* plants after pretreatment via infiltration with a 1 µM solution of flg22 24 hours prior to infection. Bars indicate samples just after inoculation (0), or 2 and 5 days after inoculation (dai). Error bars indicate SD, n = 6. **d,** Different letters represent significant differences (one-way ANOVA followed by Tukey's test corrections for multiple comparisons; $P < 0.05$). Experiments were repeated three times independently, with similar results.

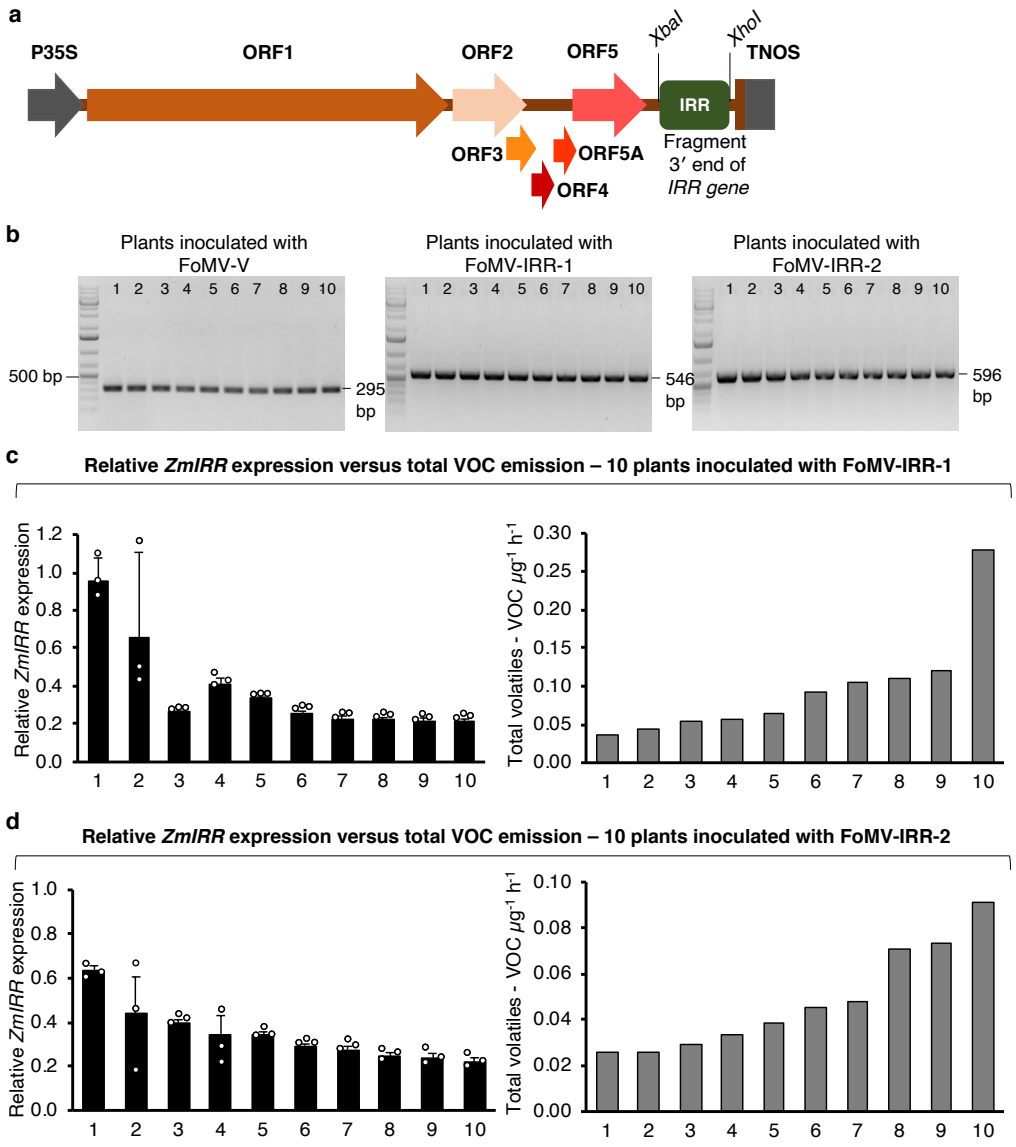

Supplementary Figure 11. Generation and analysis of maize plants carrying Zm-IRR targeting Foxtail Mosaic Virus-derived silencing constructs. a, Schematic representation of the FoMV infectious clone with *Xba*I and *Xho*I restriction enzyme sites for insertion of 251-bp or 301-bp fragments corresponding to the 3′ end of the *IRR gene* for silencing. **b,** Confirmation of FoMV infection in B73 maize plants. RT-PCR amplification across the FoMV cloning site from plants biolistically inoculated with FoMV-V, FoMV-IRR-1 and FoMV-IRR-2. FoMV-V, empty vector that carries no insert; FoMV-IRR-1 and FoMV-IRR-2, FoMV-V vector that carries IRR fragments 1 and 2, respectively. 1 to 10, RT-PCR amplification from ten individual plants. **c,** Relative expression of *ZmIRR* versus total VOC emission from leaves of B73 maize plants inoculated with virus carrying FoMV-IRR-1. **d,** Relative expression of *ZmIRR* versus total VOC emission from leaves of B73 maize plants inoculated with virus carrying FoMV-IRR-2. Relative expression of *ZmIRR* was determined by real-time qRT-PCR using mRNA from leaf 5 and *ZmRPL17* as reference gene. Error bars indicate the SD of three samples. For the total volatile organic compounds (VOC) analysis, leaf five of maize plants was treated with a 5 µM solution of ZmPep3 for 16 hours. Experiments in b-d were repeated two times independently, with similar results.

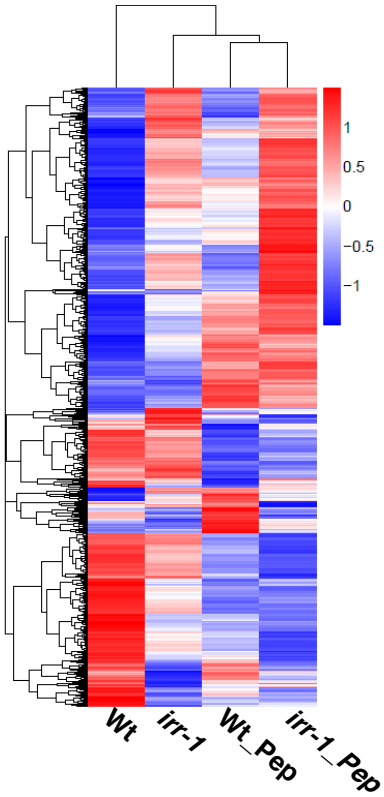

Supplementary Figure 12. Cluster analysis of differentially expressed genes in *irr-1* plants. Heat map of differentially expressed genes in wild-type (Wt) and *irr-1* plants as determined using RNA-Seq. Samples (columns) and genes (rows) are hierarchically clustered via Pearson correlation. In the clusters, 2384 genes are represented. The overall results of FPKM (fragments per kilobase of exon model per million reads mapped) cluster analysis, clustered using the $\log_{10}$(FPKM+1) value. Red denotes genes with high expression levels, and blue denotes genes with low expression levels. The color range from red to blue represents the $\log_{10}$(FPKM+1) value from large to small.

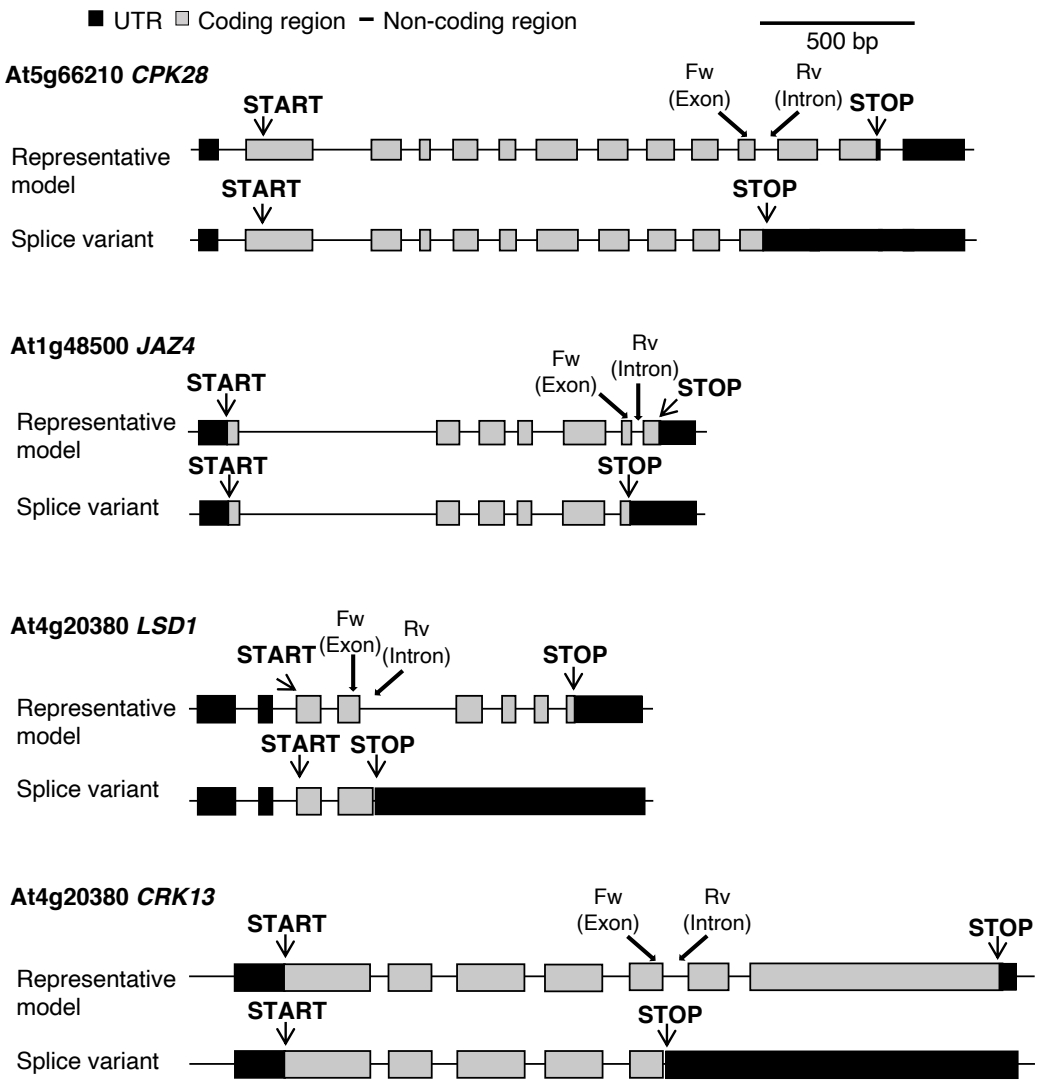

Supplementary Figure 13. Representative models and retained intron splice forms of the genes *CPK28*, *LSD1*, *JAZ4* and *CRK13*. The coding region of each gene is shown with START and STOP codons indicated. Introns are designated as a line, exons as boxes, with gray areas indicating protein coding regions, and black indicating untranslated regions (UTR). Canonical gene models and alternative splice forms were annotated by NCBI.

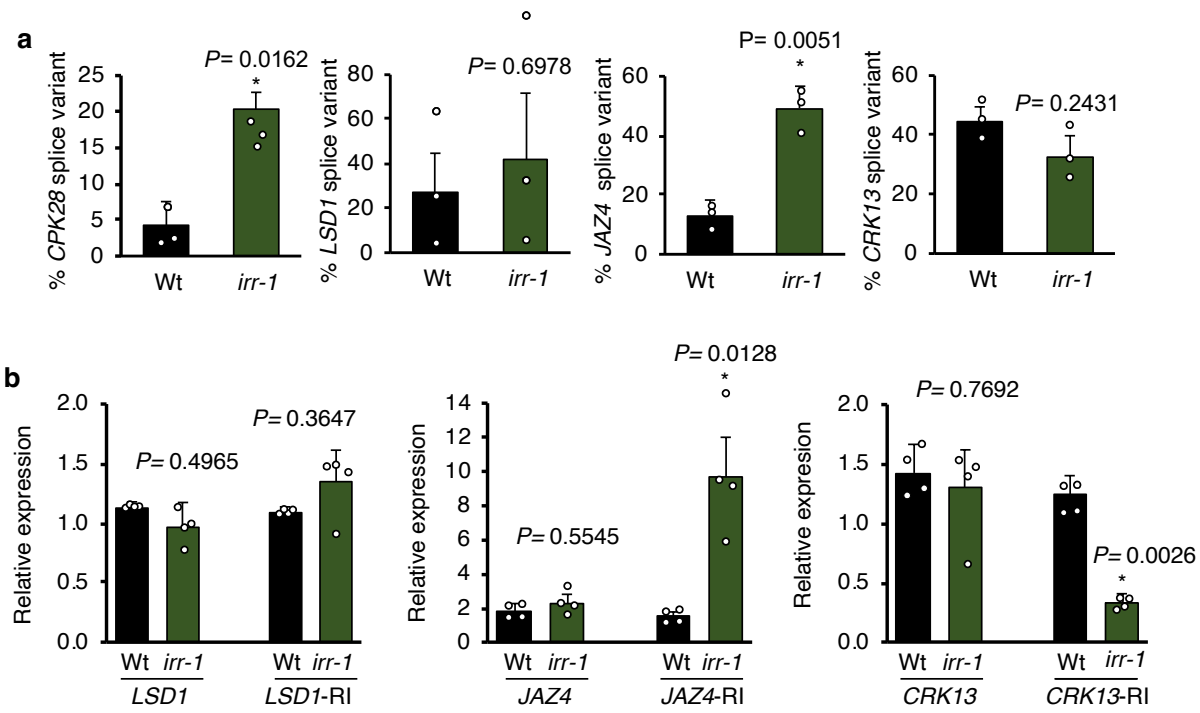

Supplementary Figure 14. Analysis of retained-intron splice variant expression for defense gene transcripts in *irr-1* knockout plants. a, Ratio of retained intron events in the transcripts *CPK28*, *LSD1, JAZ4* and *CRK13*, as determined by RNA-seq experiment. **b,** Validation of retained intron events in wild-type (Wt) and *irr-1* plants analyzed by qRT–PCR. Values represent the fold change in isoform expression versus Wt after normalization against *ACTIN2* expression. The asterisk indicates significant differences using Student t-tests (two-tailed distribution, unpaired), with $P < 0.05$.

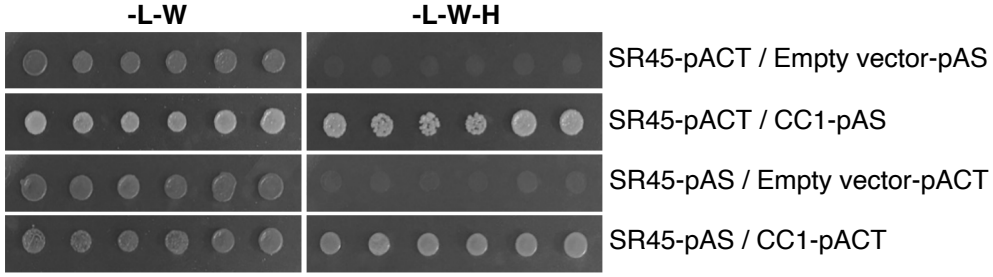

Supplementary Figure 15. SR45 protein interacts with CC1-splicing factor in yeast. SR45 interacts with CC1-splicing factor encoding protein. Yeast strain AH109 was co-transformed with desired combinations of vectors pACT and pAS carrying genes of interest. The transformants were selected in media lacking leucine and tryptophan (-L-W), and interaction was tested in media lacking leucine, tryptophan and histidine (-L-W-H). This experiment was repeated three times independently, with similar results.

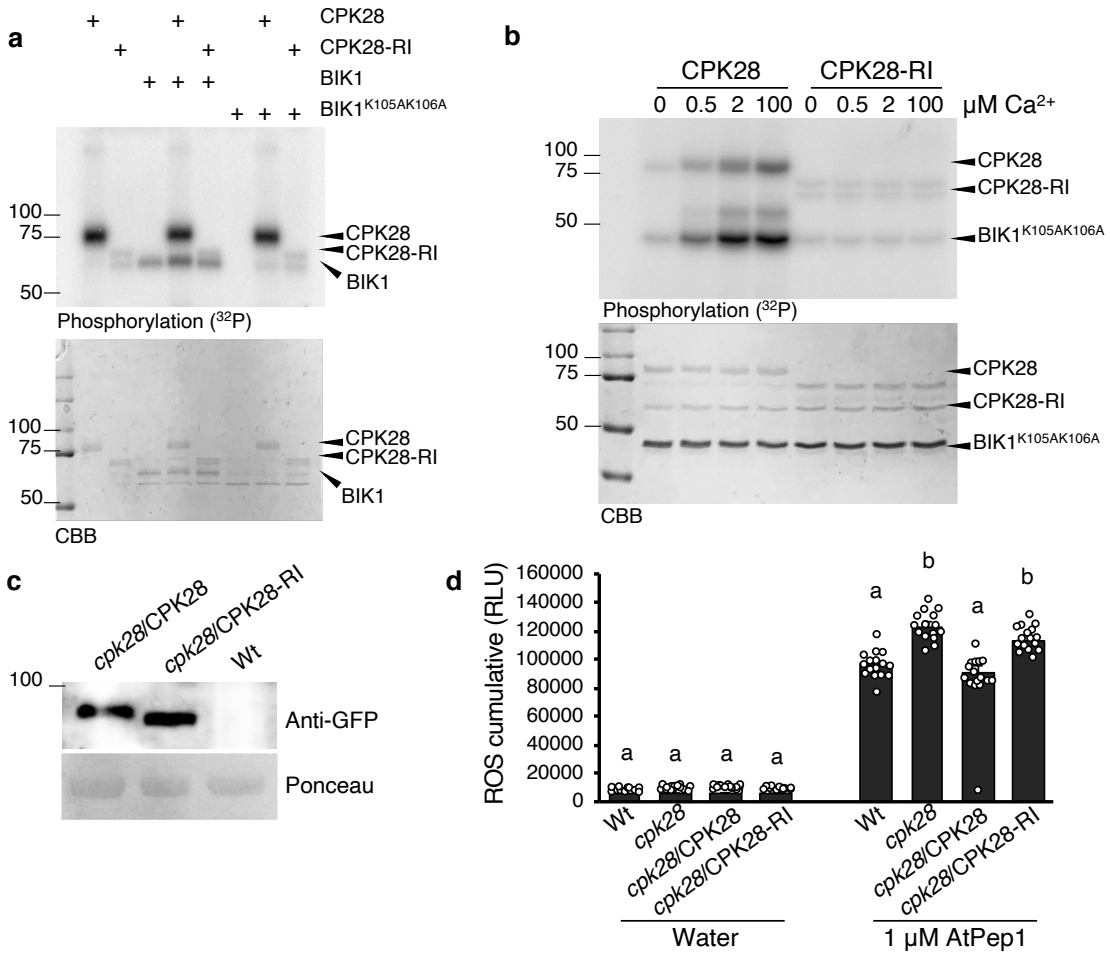

Supplementary Figure 16. Analysis of CPK28-RI protein activity. a, Autoradiograph showing incorporation of radioactive phosphate in the GST-fused CPK28, CPK28-RI and BIK1 recombinant proteins following *in vitro* kinase assays. **b,** Autoradiograph showing incorporation of radioactive phosphate in the GST-fused CPK28 and CPK28-RI and His-fused BIK1^{K105AK106A} recombinant proteins following *in vitro* kinase assays using varying concentrations of Ca^{2+}. Coomassie Brilliant Blue (CBB) stains are included as controls. **c,** Detection of CPK28-YFP and CPK28-RI-YFP fusion proteins by western blot. Proteins were extracted from leaves of transgenic plants expressing pCPK28-CPK28-YFP and pCPK28-CPK28-RI-YFP in *cpk28* background. Anti-GFP antibody was used to detect both proteins. CPK28-YFP, 85 kDa; CPK28-RI-YFP, 75 kDa. Ponceau staining was used for verification of protein loading. **d,** Total ROS production was registered continuously using luminol fluorescence for 40 min after addition of 1 µM AtPep1, then summed, n = 16, error bars represent SEM. Different letters represent significant differences (one-way ANOVA followed by Tukey's test corrections for multiple comparisons; $P < 0.05$). Experiments were repeated three times independently, with similar results.

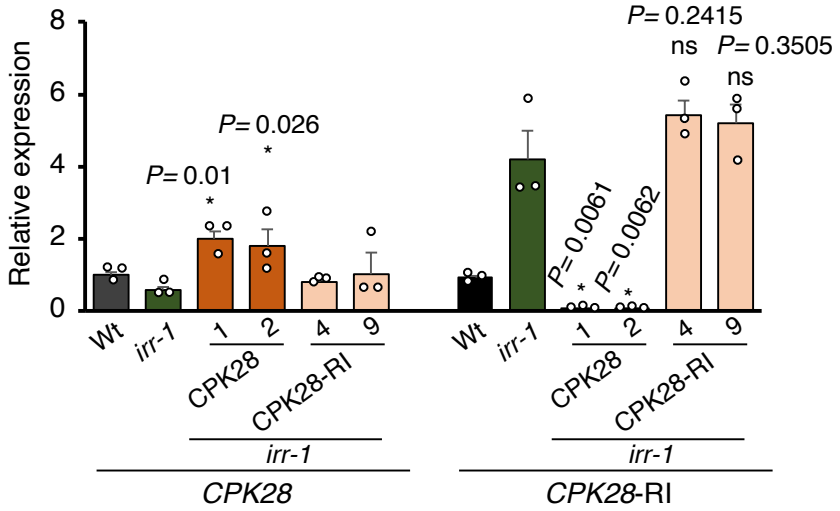

Supplementary Figure 17. *CPK28* transcript levels in *irr-1* complemented lines. The relative expression of *CPK28* and *CPK28*-RI splice variant in *irr-1* lines complemented with pCPK28:CPK28-GFP (CPK28) and pCPK28:CPK28-RI-GFP (CPK28-RI) was analyzed by qRT-PCR. Values represent the fold change in expression versus the wild-type (Wt) control samples after normalization against *ACTIN2* expression. Error bars indicate SEM. n=3. The asterisk indicates significant differences compared to *irr-1*, using Student t-tests (two-tailed distribution, unpaired), with $P < 0.05$. Experiments were repeated at least two times independently, with similar results.

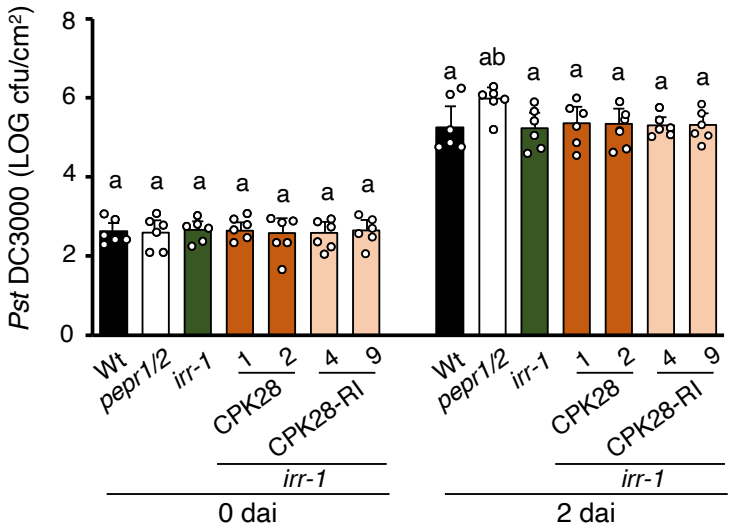

Supplementary Figure 18. Basal resistance of *irr-1*/pCPK28:CPK28-GFP transgenic lines to the bacterial pathogen *Pst* DC3000. Infection assay of *irr-1* complemented with pCPK28:CPK28-GFP (CPK28) and pCPK28:CPK28-RI-GFP (CPK28-RI). Wild-type (Wt), *irr-1* mutant and *pepr1/pepr2* (*pepr1/2*) double mutant were used as controls. Bars indicate samples 0 and 2 days after inoculation (dai). Error bars indicate SD, n = 6. Different letters represent significant differences (one-way ANOVA followed by Tukey's test corrections for multiple comparisons; $P < 0.05$). Experiments were repeated three times independently, with similar results.

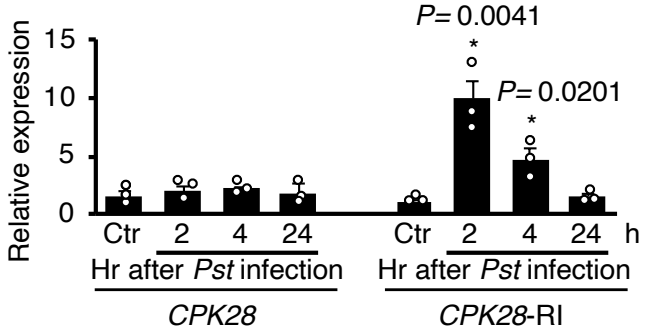

Supplementary Figure 19. Inoculation with the pathogen *Pst* DC3000 induces accumulation of *CPK28*-RI. Relative expression of *CPK28* and *CPK28*-RI splice variant transcripts in wild-type plants after *Pst* DC3000 infection, analyzed by qRT-PCR. Values represent the fold change in expression versus the uninfected control samples after normalization against *ACTIN2* expression. Plants were infected with *Pst* DC3000, and the analysis was performed 2, 4 and 24 hours (hr) after infection. Non-infected plants were used as control (Ctr). Error bars indicate SEM. n=3. The asterisk indicates significant differences using Student t-tests (two-tailed distribution, unpaired), with $P < 0.05$. This experiment was repeated three times independently, with similar results.

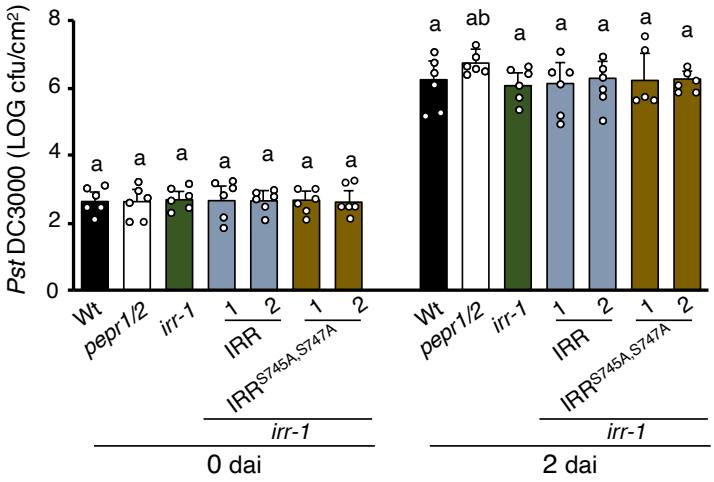

Supplementary Figure 20. Basal resistance of *irr-1*/p35S:IRR^{S745A,S747A} transgenic lines to the bacterial pathogen *Pst* DC3000. Infection assay of *irr-1* overexpressing triple HA-tagged IRR (*irr-1*:IRR) and IRR^{S745A,S747A} (*irr-1*:IRR^{S745A,S747A}). Wild-type (Wt), *irr-1* mutant and *pepr1/pepr2* (*pepr1/2*) double mutant were used as controls in assays. Bars indicate samples 0 and 2 days after inoculation (dai). Error bars indicate SD. n=6. Different letters represent significant differences (one-way ANOVA followed by Tukey's test corrections for multiple comparisons; $P < 0.05$). Experiments were repeated three times independently, with similar results.

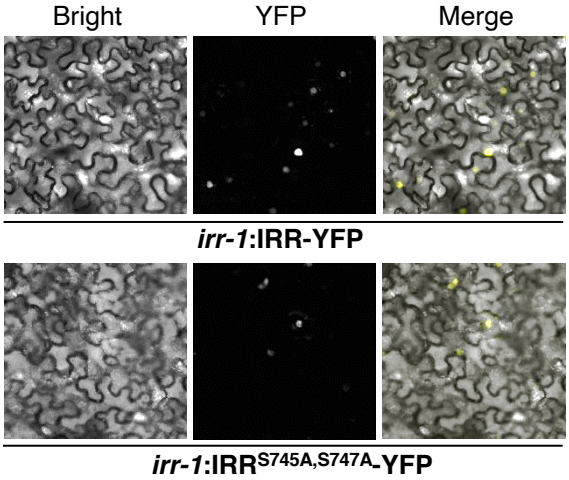

Supplementary Figure 21. Evaluation of localization of IRR-YFP versus phosphoabolishing mutant IRR^{S745A,S747A} -YFP. Visualization of YFP-tagged proteins IRR and IRR^{S745A,S747A} in cells of *Nicotiana benthamiana* four days after infiltration with *Agrobacterium*.

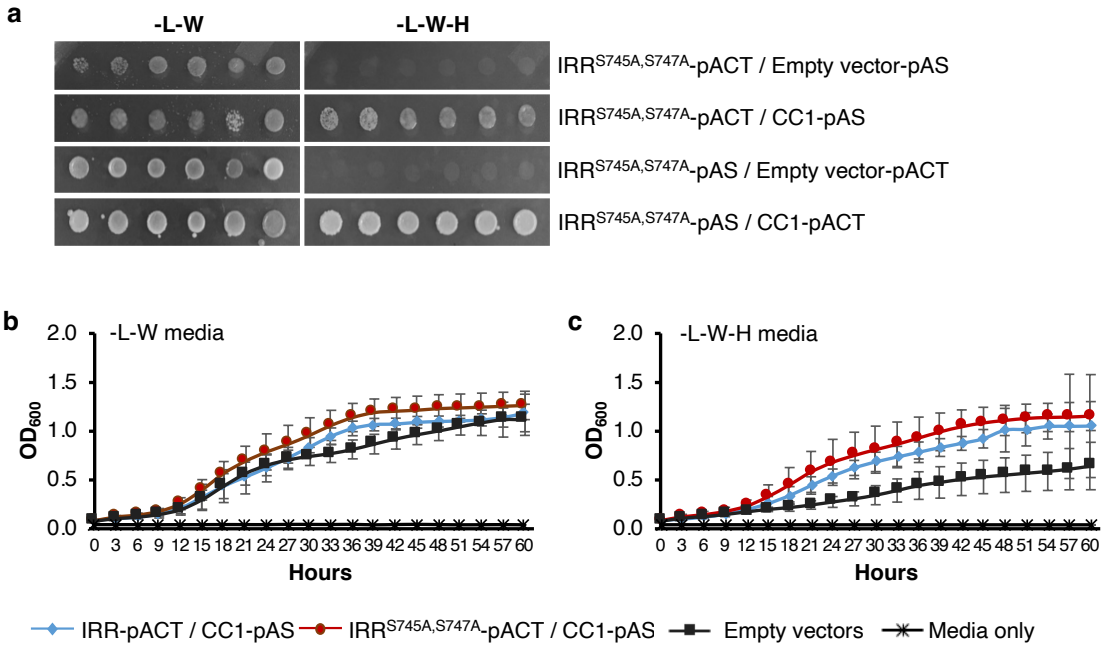

Supplementary Figure 22. IRR and IRR^{S745A,S747A} proteins interact similarly with CC1-splicing factor in yeast. a, IRR^{S745A,S747A} interacts with CC1-splicing factor. **b,** Yeast growth curve in -L-W media. **c,** Yeast growth curve in -L-W-H media. Yeast strain AH109 was co-transformed with desired combinations of vectors pACT and pAS carrying genes of interest. The transformants were selected in media lacking leucine and tryptophan (-L-W), and interaction was tested in media lacking leucine, tryptophan and histidine (-L-W-H). Experiments in a-c were repeated three times independently, with similar results.

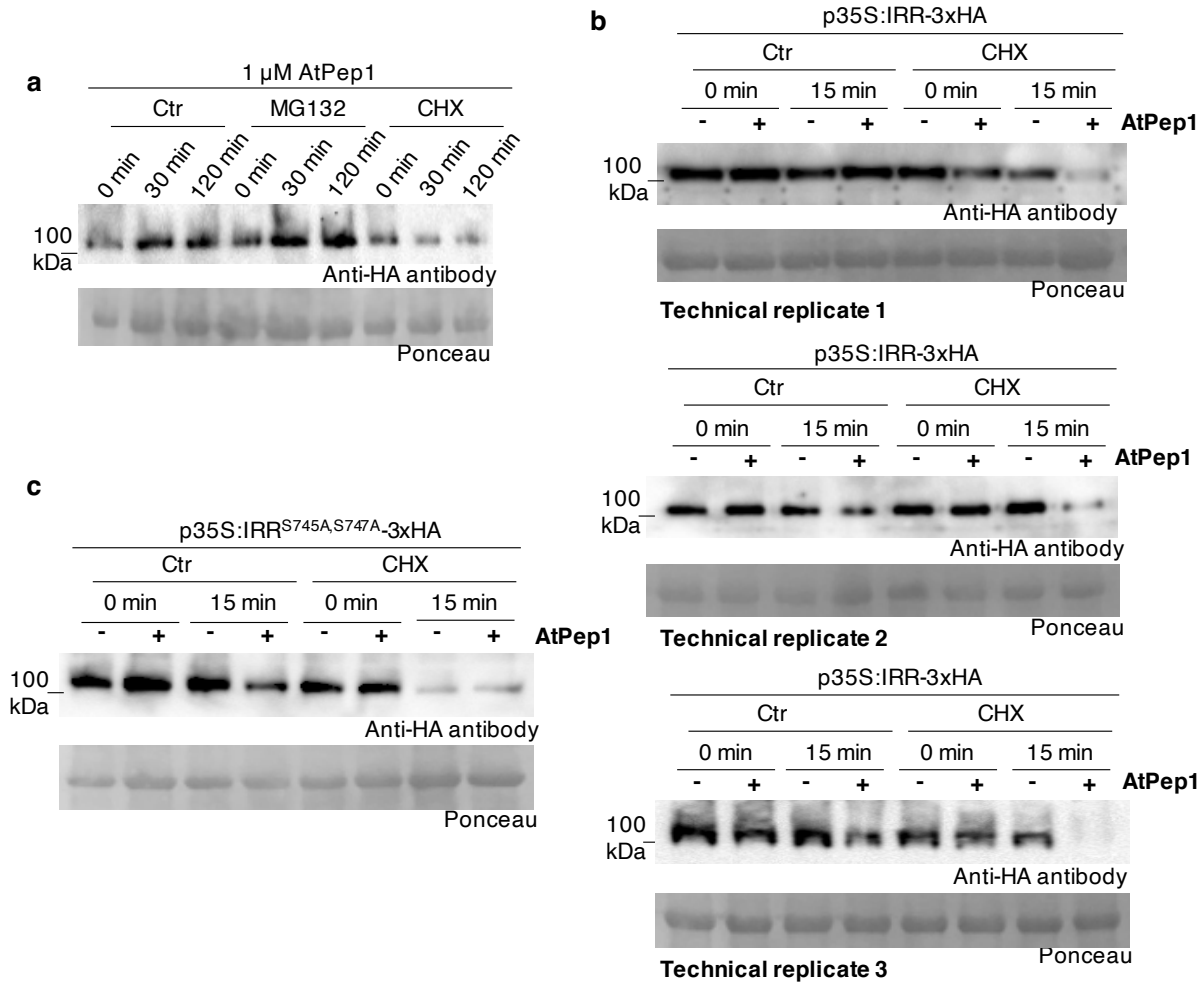

Supplementary Figure 23. AtPep1 affects stability of IRR. a, Transgenic *irr-1* plants overexpressing IRR-3xHA plants were treated with AtPep1 (1µM) and MG132 (50µM), or treated with AtPep1 (1µM) and cycloheximide (CHX; 10µM) for 0, 30 or 120 min. **b** p35S:IRR-3xHA plants were treated with water (-) or a 1 µM solution of AtPep1 (+) and cycloheximide (CHX; 10µM) for 0 or 15 min. Three technical replicates are shown. **c,** p35S:IRR-^{S745A,S747A}-3xHA plants were treated with water (-) or a 1µM solution of AtPep1 (+) and cycloheximide (CHX; 10µM) for 0 or 15 min. The solvent DMSO was used as control (Ctr). After treatments, the total protein was isolated from entire seedlings. IRR protein was subjected to immunoblot analysis with anti-HA antibody. Ponceau staining was used to visualize protein loading. Experiments were repeated at least two times independently, with similar results.

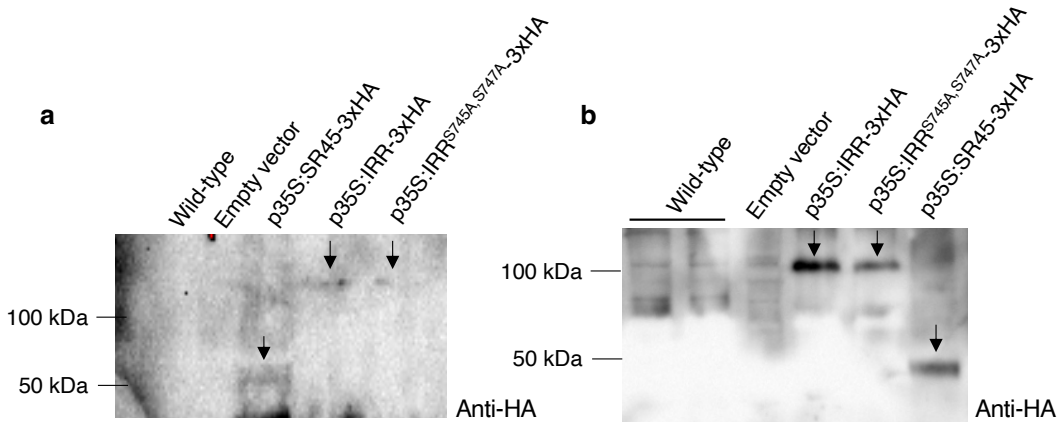

Supplementary Figure 24. Western blot detection of proteins from protein-RNA complex immunoprecipitation. The immunoprecipitation of SR45 and IRR proteins was performed with anti-HA magnetic beads with detection using anti-HA antibody. An aliquot of immunoprecipitated extract per sample was loaded for analysis: (**a**) 10 µl and (**b**) 40 µl, with relevant bands denoted by arrows.

3. Supplementary References

73. Sparkes, I. A., Runions, J., Kearns, A. & Hawes, C. Rapid, transient expression of fluorescent fusion proteins in tobacco plants and generation of stably transformed plants. *Nature protocols* **1,** 2019 (2006).

74. Clough, S. J. & Bent, A. F. Floral dip: a simplified method for *Agrobacterium* -mediated transformation of *Arabidopsis thaliana*. *The Plant journal: for cell and molecular biology* **16,** 735–743 (1998).

75. Alonso, J. M. *et al.* Genome-wide insertional mutagenesis of *Arabidopsis thaliana*. *Science* **301,** 653–657 (2003).

76. Murashige, T., Scholar, F. S. G. A revised medium for rapid growth and bioassay with tobacco tissue culture. *Phisiologia Plantarum* **15***,* 473–497 (1962).

77. Jones, D. T., Taylor, W. R., Bioinformatics, J. T. The Rapid generation of mutation data matrices from protein sequences. *Bioinformatics* **8**, 275–282 (1992).

78. Kumar, S., Stecher, K. T. MEGA7: Molecular Evolutionary Genetics Analysis Version 7.0 for Bigger Datasets. *Molecular Biology and Evolution* **33**, 1870–1874 (2016).

79. Smith, J. M. & Heese, A. Rapid bioassay to measure early reactive oxygen species production in Arabidopsis leave tissue in response to living *Pseudomonas syringae*. *Plant Methods* **10,** 6 (2014).

80. Berr, A. *et al.* Arabidopsis Histone Methyltransferase SET DOMAIN GROUP8 Mediates Induction of the Jasmonate/Ethylene Pathway Genes in Plant Defense Response to Necrotrophic Fungi. *Plant physiology* **154,** 1403–1414 (2010).